



# Kettle holes reflect the biogeochemical characteristics of their catchment area and the intensity of the element-specific input

Kai Nils Nitzsche<sup>1,9</sup> · Andreas Kleeberg<sup>2</sup> · Carsten Hoffmann<sup>1</sup> · Christoph Merz<sup>1,3</sup> · Katrin Premke<sup>4,10</sup> · Arthur Gessler<sup>5,6</sup> · Michael Sommer<sup>1,7</sup> · Zachary E. Kayler<sup>8</sup>

Received: 28 July 2021 / Accepted: 20 January 2022 / Published online: 3 February 2022  
© The Author(s), under exclusive licence to Springer-Verlag GmbH Germany, part of Springer Nature 2022

## Abstract

**Purpose** Kettle holes are small inland water bodies known to be dominated by terrigenous material; however, the processes and structures that drive the enrichment and depletion of specific geochemical elements in the water column and kettle hole sediment remain unclear. We hypothesized that the mobile elements (Ca, Fe, K, P) behave different from each other in their transport, intermediate soil retention, and final accumulation in the kettle hole sediment.

**Methods** Topsoils from transects spanning topographic positions from erosional to depositional areas, sediment cores, shallow groundwater, and kettle hole water of two glacial kettle holes in NE Germany (Rittgarten (RG) and Kraatz (KR)) were collected. The Fe, Ca, K, and total P (TP) concentrations were quantified and additionally the major anions in shallow groundwater and kettle hole water. The element-specific mobilization, relocation, and, finally, accumulation in the sediment were investigated by enrichment factors. Furthermore, a piper diagram was used to estimate groundwater flow directions and pond-internal processes.

**Results** At KR only, the upper 10 cm of the kettle hole sediment reflected the relative element composition of the eroded terrestrial soils. The sediment from both kettle holes was enriched in Ca, Fe, K, and P compared to topsoils, indicating several possible processes including the input of clay and silt sized particles enriched in these elements, fertilizer input, and pond-internal processes including biogenic calcite and hydroxyapatite precipitation, Fe–P binding (KR), FeS<sub>x</sub> formation (RG), and elemental fixation and deposition via floating macrophytes (RG). High Ca concentrations in the kettle hole water indicated a high input of Ca from shallow groundwater inflow, while Ca precipitation in the kettle hole water led to lower Ca concentration in groundwater outflow.

**Conclusions** The considerable element losses in the surrounding soils and the inputs into the kettle holes should be addressed by comprehensive soil and water protection measures, i.e., avoiding tillage, fertilizing conservatively, and creating buffer zones.

**Keywords** Agricultural soils · Soil erosion · Element mobility · Phosphorus · Kettle hole · Sediment

## 1 Introduction

Over the past decades, the coupling of physical and biogeochemical dynamics of small inland water bodies have received little attention compared with larger and deeper systems (Branco and Torgersen 2009). While large water bodies

receive much less terrestrial material in sum compared to their volume, small water bodies are known to be dominated by terrigenous material (Biddanda and Cotner 2002). Sediment cores provide integrating information on the natural and anthropogenic changes in the catchment; however, few data exist for small water bodies.

The agricultural landscape of NE Germany is characterized by a high density of kettle holes, which are small (< 1 ha), pond-like depressional wetlands (Kalettka and Rudat 2006). These small and very shallow water bodies widely occur in glacial landscapes of the Northern Hemisphere (Tiner 2003; van der Kamp and Hayashi 2009;

---

Responsible editor: Marcel van der Perk

---

✉ Kai Nils Nitzsche  
kai.nitzsche@jamstec.go.jp

Extended author information available on the last page of the article

Goldyn et al. 2015). They are hotspots of biodiversity in agricultural landscapes (e.g., Kalettka et al. 2001); thus, in Germany, they are protected by law. However, in the agricultural landscape of NE Germany, where many kettle holes are located, soil erosion by water and tillage operations due to widespread land clearance and agricultural intensification has led to significant soil translocation (Deumlich et al. 2006; Gericke et al. 2019) and increased sedimentation rates (Kleeberg et al. 2016a). As basins without outlets, kettle holes can be regarded as ultimate sinks for all matter (organic matter, nutrients, soil, contaminants) originating from their catchments. Thus, kettle holes located in agricultural fields receive non-point-source input of agricultural pollutants and eroded soil from their closed watersheds (Frielinghaus and Vahrson 1998).

The physical process of soil erosion mobilizes base cations (e.g., Ca, Mg, K, Na), heavy metals (e.g., Fe), and biogenic elements (C, N, P) downslopes, where they are deposited as colluvial material (Gaspar et al. 2020). However, a significant part of eroded soil material is transported from terrestrial slopes, into the kettle hole water and finally accumulates as kettle hole sediment. The extent of mobilization, transport, deposition and accumulation are element- and site-specific (Prasad et al. 2005). While conservative elements (e.g., K and Mg) hardly interact with structures (soil, vegetation, groundwater, interflow), redox-sensitive elements (e.g., Fe) can precipitate as immobile oxides or sulfides and can be mobilized based on Eh (redox potential) and/or pH changes, and biogenic elements (e.g., P) repeatedly cycle between the biosphere and pedosphere before final accumulation and burial in the kettle hole sediment (Li et al. 2012; Farkas et al. 2013; Haygarth et al. 2013). Transport processes of these diverse elements in the catchment area can be identified by field surveys by relating elemental enrichments and depletions. However, between mobilization and accumulation a large number of processes occur through different landscape filters, i.e., intermediate deposition of soil material at mid- or downslopes, various structures (e.g., vegetation), and abiotic and/or biotic processes in the water column and sediment. Consequently, it is not clear which processes and structures drive the enrichment and depletion of specific elements in the sediment and in the kettle hole water on a short scale and within short periods of time. Furthermore, evidence exists for at least temporal connection of the kettle holes to shallow groundwater systems (Lischeid et al. 2017; Nitzsche et al. 2017a; Kayler et al. 2018; Vyse et al. 2020). Thus, the water quality of kettle holes might also be strongly affected by the groundwater system (Lischeid et al. 2018).

Two glacial kettle holes near the villages of Kraatz (KR) and Rittgarten (RG), NE Germany, were selected as representative for a wide range of small inland water bodies based on their size (Fig. S1) in terms of morphological, vegetation

related, and hydrological features (Premke et al. 2016). Moreover, these kettle holes are intensively studied with regard to organic matter distribution and retention (Nitzsche et al. 2017b), elemental contents and soil organic and mineral matter composition (Leue et al. 2019), sedimentation (Kleeberg et al. 2016a), sediment core stratigraphy (Kleeberg et al. 2016b), primary production (Kazanjian et al. 2018), carbon and nutrient cycling (Attermeyer et al. 2017; Revery et al. 2018), and biogeochemical modeling (Onandia et al. 2018). The role of both land use impacts (Nitzsche et al. 2016) and hydroperiod on kettle hole biogeochemistry was also studied (Nitzsche et al. 2017a).

The aim of this study was to characterize the coupling of geogenic and aquatic processes in the two small catchment areas including small inland water bodies, based on the investigation of the element-specific mobilization, relocation, and final accumulation in the sediment of the kettle hole. We hypothesize that the elements considered (Ca, Fe, K, P) that are mobilized in the catchment area behave differently from each other in their transport, intermediate retention, and final accumulation in the kettle hole sediment. Characterizing the specific loss of elements from the catchment to the adjacent water body is crucial for understanding potential long-term negative consequences for farming and the trophic state of kettle holes. Furthermore, based on this process understanding, we can approach a comprehensive picture of soil redistribution and erosion processes within the two catchments.

## 2 Material and methods

### 2.1 Study site

Both kettle holes, at Kraatz (KR) and Rittgarten (RG) are located in the Uckermark region, which belongs to the young and hummocky moraine plain, NE Germany. This landscape was formed after the end of the Weichsel glaciation (~ 10 k years BP), and contains up to 300,000 of these kettle holes (Kalettka and Rudat 2006).

The morphometric characteristics of the kettle holes of their catchments are summarized in Table 1. The kettle hole KR is surrounded by *Salix cinerea* L. shrubs and populated by a mixture of submerged, emergent, and floating macrophytes (Kazanjian et al. 2018). The KR catchment is characterized by loamy soils with a medium to high exposure to erosion. Calcaric Regosols (caRG) and Calcic Luvisols (eLV) prevail on hilltops and along upper slopes. At foot-slopes around the water body, Colluvic Regosols (coRG) with colluvial M-horizons thicker than 50 cm are found (Leue et al. 2019), which develop under groundwater and stagnant water conditions (Gleysols (GG), Stagnosols).

**Table 1** Morphometric characteristics of the kettle holes at Kraatz and at Rittgarten and of their catchments

	Kraatz	Rittgarten
Catchment size (ha)	3.4	3.1
Elevation in the catchment (m)	88.2 to 101.1	74.5 to 77
Volume (m <sup>3</sup> )	1797	3998
Area (m <sup>2</sup> )	2689	1459
Maximum depth (m)	2.64	2.34
Mean depth (m)	1.48	1.23

The kettle hole RG is 5 km away from KR and is surrounded by a reed belt comprising of *Phragmites australis* (Cav.) Trin. ex Steud. Furthermore, it is fully covered by non-rooted submerged *Ceratophyllum submersum* L. and floating macrophytes *Lemna minor* L., *Spirodela polyrhiza* (L.) Schleid during the summer months (Kazanjian et al. 2018). Sandy soils with low to medium exposure to erosion prevail. Albic and Haplic Regosols dominate on upper slopes, while Colluvic Gleysols were present around the water body.

Both catchments are in agricultural use for several centuries. From 1990 on, both fields were cultivated rotationally by winter wheat (*Triticum aestivum* L.), winter barley (*Hordeum vulgare* L.), and rapeseed (*Brassica napus* L.). Annual plowing was common until 2005 at a depth up to 30 cm; thereafter, soils were ploughed every third year. Calcium (via liming), K and P (via pig slurry) have been applied and removed with crops (Table 2). Liming was common until 2010 for winter wheat. In years with winter wheat and rapeseed cultivation, a manure slurry from a nearby pig farm was applied since 1990. The climate is sub humid with an average annual air temperature of 8.6 °C, and an average annual precipitation of 499 mm between 1992 and 2013 (AgroScapeLab Quillow, Dedelow).

## 2.2 Sampling of soils, sediments, kettle hole water, and shallow groundwater

For general pedological field characterization of the areas (e.g., soil texture by finger test, redoximorphic features, and

**Table 2** Yearly Ca, K, and total P (TP) inputs via liming (Ca) and pig slurry application (K, TP) when averaging 3 years, and removal with crops based on crop yields in the area

Parameter	Input via fertilization	Removal with crops
Ca (kg ha <sup>-1</sup> year <sup>-1</sup> )	400	8
K (kg ha <sup>-1</sup> year <sup>-1</sup> )	85	35
TP (kg ha <sup>-1</sup> year <sup>-1</sup> )	45	30
Fe (kg ha <sup>-1</sup> year <sup>-1</sup> )	In traces	In traces

carbonates contents), 1-m depth soil cores (Pürckhauer boring), which were spatially widely distributed, were taken from the two catchments. The distribution and thickness of characteristic soil horizons was recorded. Based on this general survey, three four-position transects were sampled at both sites (Fig. 1). Samples of topsoil material (0–15 cm) from the two kettle hole catchments were collected in May 2013. Owing to the steeper topographic gradient at KR, the sample locations can be characterized based on their slope positions (hilltop, hillslope, foot slope, depression edge). Owing to the flat topography at RG, no visual hilltops exist but light undulating flat ridge settings. Therefore, the topography was grouped and sampled in flat ridge, footslope, and depressional edges. At each sampling position, we took three subsamples of 100 g soil in a 1 m<sup>2</sup> area and mixed the samples afterward. Soil samples were air-dried and passed through a 2 mm sieve prior to further analyses. At sampling points, soil profiles were classified according to IUSS Working Group WRB (2015).

Sediment sampling was described elsewhere (Kleeberg et al. 2016b). Briefly, two undisturbed sediment cores (6-cm diameter) were taken at the maximum depth in each kettle hole using a UWITEC<sup>®</sup> (Mondsee, Austria) corer on 19 June 2013. The RG<sub>1</sub> core was 31 cm long, and the KR<sub>1</sub> was 51 cm long. These cores were used for the determination of metal concentrations. The two additional sediment cores (RG<sub>2</sub> 29 cm long, KR<sub>2</sub> 54 cm long) were taken at the same sites on 10 October 2013 for dating and other analyses.

In October 2013, four groundwater observation wells were installed at each kettle hole. The groundwater wells (2-inch pipes made of PE with 1 m filter screen) were installed down to 2–3 m depth at maximum (down to 4 m at one well only at RG) around each kettle hole close to the shoreline. Shallow groundwater was sampled monthly using a submersible pump from February 6 to June 11 2014. Due to falling water tables, observation wells < 2.5 m fell dry in April. In early summer 2014, all groundwater wells fell dry.

Kettle hole surface water was sampled bi-weekly between July 4, 2013, and July 22, 2014. Kettle hole water and shallow groundwater samples were filtered (0.45 µm) and cooled at 4 °C before further analysis.

## 2.3 Chemical analyses

The content of soil organic carbon (SOC) and total inorganic C (TIC) of soil samples were analyzed in ground soil samples using a RC612 multiphase C/N analyzer (LECO Corporation, Michigan, USA) according to ISO 10694 (1995). The TOC of sediment cores RG<sub>2</sub> and KR<sub>2</sub> was estimated as organic matter (OM) × 0.5 (Brenner and Binford 1988) after the proportion of OM was determined as loss on ignition (LOI) at 450 °C for 3 h. The concentrations of Al, Fe, Mg, Ca, K, Na, and total P (TP) were determined

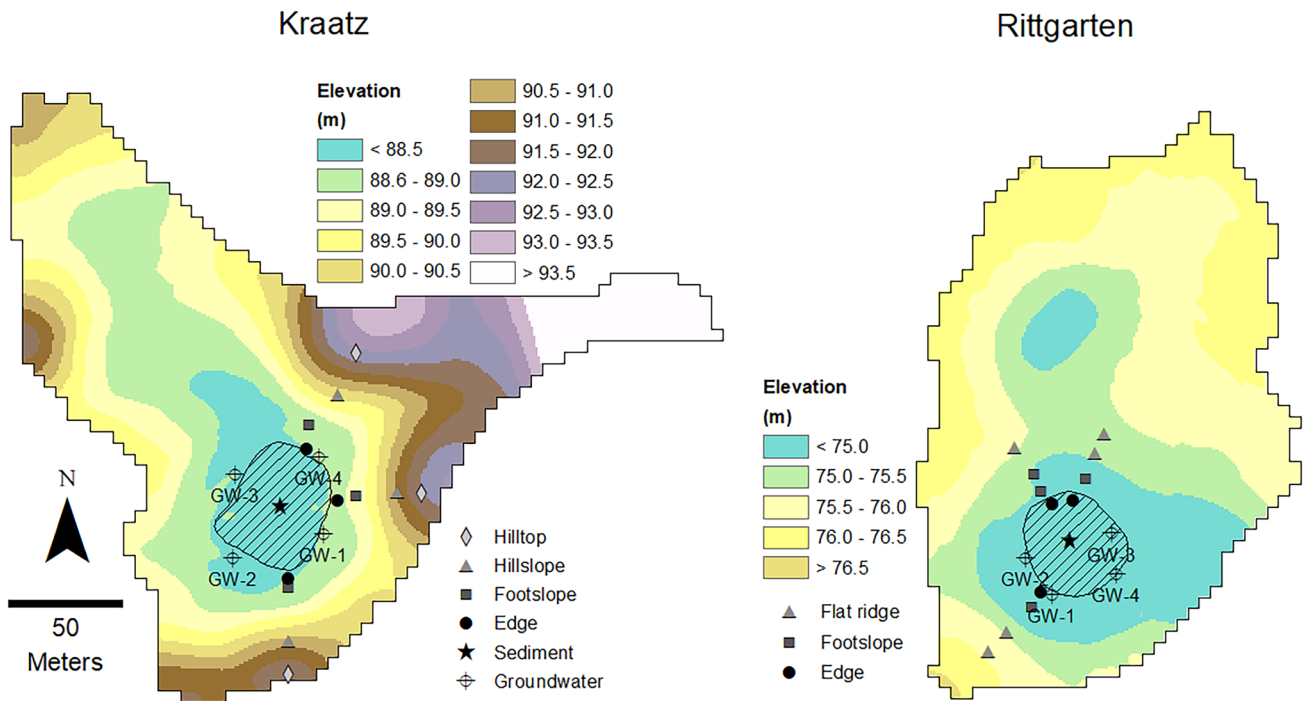


**Fig. 1** Elevation models of the kettle hole catchments Kraatz (KR) and Rittgarten (RG) with sampling locations of soils, sediments, and shallow groundwater

by inductively coupled plasma optical emission spectrometry (ICP-OES, ICP-iCAP 6300 DUO Thermo Scientific, Bremen) after wet digestion of dry, weighed samples in aqua regia (HCl:HNO<sub>3</sub> 3:1) in a microwave (1600 W, 160 °C, 20 min).

Metal determination of sediment is described elsewhere (Kleeberg et al. 2016b). Briefly, metal concentrations at 500- $\mu$ m resolution were determined along the core by micro-X-ray fluorescence ( $\mu$ XRF) using an ITRAX core scanner (Cox Analytical Instruments, Mölndal, Sweden). The other core half was sliced into 1-cm intervals that were analyzed by conventional methods to convert the semi-quantitative  $\mu$ XRF data (counts) into concentrations [ $\text{mg g}^{-1}$  dry weight (dw)] by correlation (Neyen 2014). Concentrations of Fe, Ca, and K were determined following the protocol used for topsoil samples. Sediment TP was determined as soluble reactive P (SRP) after wet acid (1 N HCl) digestion of the ash from the OM determination according to Andersen (1976).

The water samples were analyzed for TP (only kettle hole water), SRP (only kettle hole water), phosphate (PO<sub>4</sub>), total N (TN), ammonium (NH<sub>4</sub>), nitrate (NO<sub>3</sub>), dissolved organic C (DOC), chloride (Cl), sulfate (SO<sub>4</sub>), and chlorophyll a (Chl a) (only kettle hole water), HCO<sub>3</sub> (only groundwater), and Ca, Fe, K, Mg, Mn, and Na, using limnological standard methods (Kleeberg et al. 2010; Lischeid and Kalettka 2012). Missing HCO<sub>3</sub> concentrations in some shallow groundwater wells during certain sampling times ( $n=12$ ) and HCO<sub>3</sub>

concentrations in the kettle hole water were estimated based on ion balance calculations.

#### 2.4 Calculation of the enrichment factor and the elemental retention

In order to understand the accumulation of metals in the sediment relative to the soil, we calculated the element(X)-specific enrichment factor  $EF_X$ , which is defined as the concentration of the element in the eroded matter divided by the concentration in the source matter (Menzel 1980). Furthermore, to quantitatively estimate the theoretical elemental input, Fe, Ca, K, and TP retention (in  $\text{g m}^{-2} \text{a}^{-1}$ ) was calculated by multiplying the respective concentration (in  $\text{mg g}^{-1}$ ) with the sedimentation rate (in  $\text{g dw m}^{-2} \text{a}^{-1}$ , from Kleeberg et al. 2016a).

#### 2.5 Estimation of erosion and deposition

Kettle hole catchments within agricultural landscapes of NE Germany have been influenced by soil erosion and deposition processes over the past decades. To get a comprehensive picture of soil distributions and erosion processes within the KR catchment, 28 soil driving cores up to 1.5 m in length were taken. Soil profiles were classified based on the World Reference Base for Soil Resources (WRB) standard (FAO 2014). Horizon thickness and names were collected for each



core. Depth profiles of Ca contents were analyzed by portable x-ray fluorescence (pXRF) spectroscopy (Leue et al. 2019). The site selection of core sampling points reflected the diversity of different topographical features such as slope, curvature, topographic wetness index (TWI), and the topographic position index (TPI, Deumlich et al. 2010).

An Albic Luvisol (initial little erosive disturbed soil profile) has been taken as reference with a C-horizon (=CaCO<sub>3</sub> rich glacial till) depth of 123 cm. The difference to the initial 123 cm was assumed to be the depth of profile shortening (at erosive sites) and lengthening (at deposition sites). At strongly eroded sites (e.g., hilltops) the glacial till was already incorporated into the Ap (plow) horizon. The higher the concentration of Ca, the stronger the erosion at this site and the more often the farmer already tilled into the CaCO<sub>3</sub> rich till. The “grade of dilution” of Ca into the Ap horizon was then used to estimate the proportion of glacial till in Ap horizon. The estimated depths of C horizon at these points were in some cases negative (erosion rate > 123 cm). In the depression, the C-horizon was not reached by driving cores but a fossil Ah horizon (fAh). The depth to the fAh indicate the amount of deposition. By this method, depths values of erosion and accumulation were measured or calculated for all 28 coring positions.

The spatial distribution of C horizon depths (1 × 1 m<sup>2</sup> grid cells) was than calculated by the CUBIST model, using all available topographic features/indexes into account, i.e., curvature, slope, TWI, and TPI.

## 2.6 Statistical analyses

The Shapiro–Wilk test was used to test for normally distributed data and the Levene’s test to test for homoscedasticity. To test whether the relative Fe, Ca, K composition of the soils, sediment, kettle hole water, and shallow groundwater were similar, a principal component analysis (PCA), using the molar Fe:Ca, Fe:K, and Ca:K ratio, was performed.

## 3 Results

### 3.1 Elemental composition of soils

At KR, the SOC concentration in topsoils increased from 6.1 to 15.7 mg g<sup>-1</sup> from hilltop toward the kettle hole (Table S1). The Fe concentration (12.3 to 23.6 mg g<sup>-1</sup>) and K concentration (6.2 to 2.4 mg g<sup>-1</sup>) decreased from the hilltops toward the kettle hole shoreline (Fig. 2). The concentration of Ca decreased from 41.4 at hilltops to 2.8 mg g<sup>-1</sup> at kettle hole edges. TP showed no trends (0.4 to 0.5 mg g<sup>-1</sup>) along the slope/catena. Owing to the large variation in Fe and Ca across the transects, the molar Fe:Ca ratio increased from 0.3 to 3.2 toward the kettle hole.

At RG, similar to KR, the SOC concentration increased from 8.0 to 12.3 mg g<sup>-1</sup> toward the kettle hole vegetation belt. The concentration of Fe, Ca, and K of soils at RG were lower compared to those at KR and remained rather constant across the transects. Fe ranged from 7.9 to 15.6 mg g<sup>-1</sup>, Ca from 1.9 to 3.0 mg g<sup>-1</sup>, and K from 1.7 to 3.8 mg g<sup>-1</sup>. Total phosphorus was in a similar range (0.4 to 0.5 mg g<sup>-1</sup>) compared to KR. In contrast to KR, the molar Fe:Ca ratio remained rather constant throughout the transects and ranged from 3.5 to 4.7.

### 3.2 Elemental composition of the kettle hole sediment

At KR, the SOC content decreased down-core from 109.4 to 31.7 mg g<sup>-1</sup> (Fig. S2), indicating the significant OC enrichment in sediment by a factor of 2 to 7 compared to upslope position. Fe remained relatively constant and ranged from 29.8 to 37.6 mg g<sup>-1</sup>, Ca from 9.8 to 4.2 mg g<sup>-1</sup>, and K from 7.6 to 5.4 mg g<sup>-1</sup>. Total P strongly decreased down-core from 4.7 to 1.4 mg g<sup>-1</sup>. The molar Fe:Ca ratio remained rather constant throughout the sediment core (2.6 to 3.7) except for maxima near the surface.

At RG, SOC content decreased downwards from 329.1 to 89.2 mg g<sup>-1</sup>. Thus, the sedimentary SOC was 7 to 27 times higher than that of surrounded topsoils. Fe showed no trend along the core transects ranging from 24.3 to 38.0 mg g<sup>-1</sup>. Ca slightly increased downwards from 5.8 to 7.1 mg g<sup>-1</sup> except for values at around 1.6 cm depth. Similar to Ca, K showed a slight downward increase from 2.2 to 3.8 mg g<sup>-1</sup>. In contrast to KR, TP remained rather constant ranging from 0.75 to 1.02 mg g<sup>-1</sup>. Similar to KR, the molar Fe:Ca ratio was constant between 1.8 to 10 cm depth ranging from 3.4 to 2.7, but decreased promptly from 4.4 at the surface to 1.8 at around 1.7 cm depth.

### 3.3 Elemental concentrations of the shallow groundwater

Shallow groundwater was not always available from all sampling locations during all sampling times (Fig. S3). At KR, the Ca, Mg, and HCO<sub>3</sub> concentrations were on average approximately two times lower than RG, but that of K was on average two times higher than RG (Table 3). Phosphate concentrations are comparable for both sites and SO<sub>4</sub> is 1.5 times higher at RG.

At KR, Ca and HCO<sub>3</sub> concentrations dominate in the shallow groundwater. Therefore, the groundwater can be classified as Ca-HCO<sub>3</sub> water. Regarding the cations, shallow groundwater monitoring sites KR-GW-1 and KR-GW-2 have higher Ca, K and Mg concentrations than KR-GW-3 and KR-GW-4 (Fig. S3). This differentiation also applies to

**Fig. 2** Content of elements Fe, Ca, K, total P (TP), the molar Fe:Ca ratio of topsoils (0–15 cm) versus the distance of the sampling position relative to the kettle hole shoreline (m) at Kraatz (KR, left panels) and Rittgarten (RG, right panels)

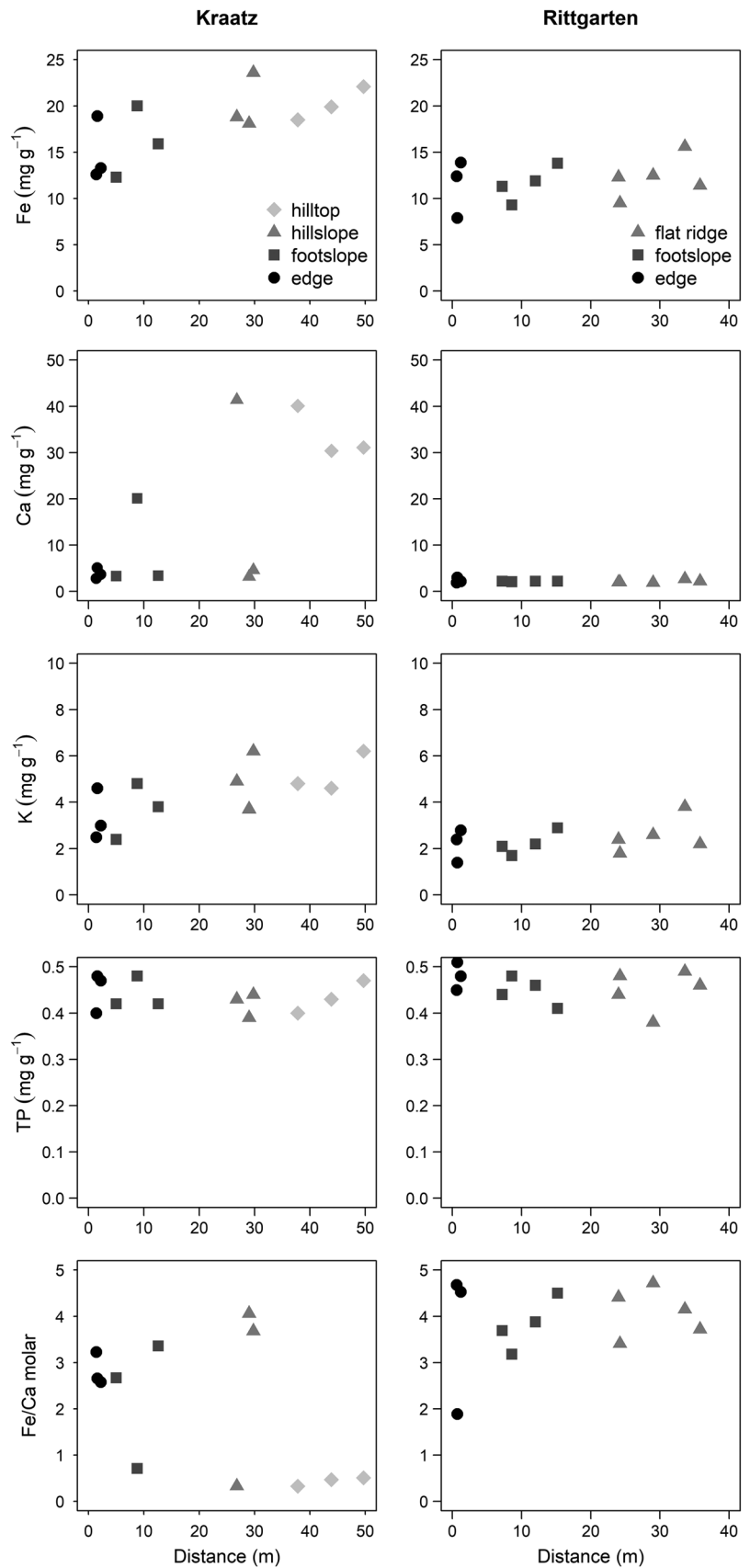


**Table 3** Mean concentration ( $\pm$ standard deviation) and span (in brackets) of shallow groundwater chemistry at Rittgarten between February and May 2014 ( $n=12$  occasions) and at Kraatz between February and June 2014 ( $n=14$  occasions)

Parameter	Kraatz	Rittgarten
Ca (mg L <sup>-1</sup> )	72.9 $\pm$ 43.9 (31.0–165.8)	146.7 $\pm$ 24.3 (120.2–190.0)
K (mg L <sup>-1</sup> )	16.7 $\pm$ 12.9 (0.8–39.9)	7.9 $\pm$ 5.0 (2.3–18.4)
Mg (mg L <sup>-1</sup> )	5.5 $\pm$ 2.7 (2.8–10.4)	12.5 $\pm$ 1.7 (10.2–15.6)
Na (mg L <sup>-1</sup> )	9.1 $\pm$ 4.3 (3.2–15.7)	15.3 $\pm$ 1.2 (13.9–17.8)
Bicarbonate (mg L <sup>-1</sup> )	222 $\pm$ 108 (92–427)	460 $\pm$ 104 (354–641)
Chloride (mg L <sup>-1</sup> )	16.0 $\pm$ 9.2 (10.0–37.5)	26.9 $\pm$ 2.0 (23.7–29.9)
Nitrate (mg L <sup>-1</sup> )	10.6 $\pm$ 19.3 (0.4–54.9)	1.4 $\pm$ 1.3 (0.1–4.3)
Ammonia (mg L <sup>-1</sup> )	0.09 $\pm$ 0.09 (0.00–0.21)	0.25 $\pm$ 0.17 (0.12–0.57)
Phosphate (mg L <sup>-1</sup> )	0.09 $\pm$ 0.06 (0.04–0.21)	0.11 $\pm$ 0.10 (0.01–0.26)
Sulphate (mg L <sup>-1</sup> )	27.5 $\pm$ 20.1 (10.6–69.2)	40.6 $\pm$ 26.1 (11.8–83.9)

the HCO<sub>3</sub> concentrations. Higher SO<sub>4</sub> concentrations can only be detected in well KR-GW-1.

At RG, the shallow groundwater can also be classified as Ca-HCO<sub>3</sub> water. The differences in cations at the shallow groundwater monitoring wells are relatively small and mainly determined by a variation of Ca concentrations. A clear differentiation is rather seen in the anions. In general, HCO<sub>3</sub> contents dominate, but with a higher variation of SO<sub>4</sub>. RG-GW-2 and RG-GW-3 are characterized by lower HCO<sub>3</sub> concentrations and relatively high SO<sub>4</sub> concentration, while the opposite applies to RG-GW-1 and RG-GW-4.

### 3.4 Elemental concentrations of the kettle hole water

At KR, Fe concentration was on average 9 times higher than that of RG (Table 4, Fig. S4). KR had an on average 2.3 times lower Ca and Mg, and 1.7 times lower TP concentration than RG. The K concentration was equal at both sites. At KR, due to its high Fe concentrations, mean molar Fe:Ca and Fe:P ratios were 18 and 8.6 times higher than at RG. Furthermore, RG had on average 5.3 times higher SRP, 2.3 times higher HCO<sub>3</sub> and two times higher SO<sub>4</sub> concentration as KR, but their NO<sub>3</sub> concentration was similar. KR had five times lower Chl a concentration than RG.

**Table 4** Mean concentration ( $\pm$ standard deviation) and span (in brackets) of water chemistry and molar ratio of Fe:Ca and Fe:P of kettle holes at Rittgarten and Kraatz between July 2013 and July 2014 ( $n=22$  occasions)

Parameter	Kraatz	Rittgarten
Ca (mg L <sup>-1</sup> )	32.9 $\pm$ 8.5 (21.4–57.6)	77.3 $\pm$ 10.9 (63.0–99.8)
Fe (mg L <sup>-1</sup> )	1.6 $\pm$ 1.2 (0.2–4.3)	0.2 $\pm$ 0.1 (0.03–0.5)
K (mg L <sup>-1</sup> )	10.5 $\pm$ 2.8 (6.2–16.0)	10.8 $\pm$ 2.5 (4.1–14.0)
Mg (mg L <sup>-1</sup> )	4.3 $\pm$ 0.6 (2.6–5.3)	9.5 $\pm$ 0.7 (8.2–10.5)
Na (mg L <sup>-1</sup> )	4.2 $\pm$ 2.2 (2.2–10.8)	11.3 $\pm$ 1.3 (9.4–13.7)
Bicarbonate (mg L <sup>-1</sup> )	116 $\pm$ 29 (61–183)	262 $\pm$ 23 (244–305)
Chloride (mg L <sup>-1</sup> )	11.8 $\pm$ 2.0 (9.5–16.1)	23.0 $\pm$ 1.7 (19.1–26.5)
Nitrate (mg L <sup>-1</sup> )	0.12 $\pm$ 0.11 (0.03–0.46)	0.10 $\pm$ 0.06 (0.00–0.27)
Ammonia (mg L <sup>-1</sup> )	0.16 $\pm$ 0.28 (0.00–1.28)	0.23 $\pm$ 0.33 (0.00–1.33)
Total P (mg L <sup>-1</sup> )	0.15 $\pm$ 0.10 (0.04–0.37)	0.26 $\pm$ 0.31 (0.03–1.10)
Phosphate (mg L <sup>-1</sup> )	0.03 $\pm$ 0.02 (0.00–0.07)	0.16 $\pm$ 0.22 (0.00–0.66)
Sulphate (mg L <sup>-1</sup> )	9.4 $\pm$ 0.8 (8.7–12.1)	18.7 $\pm$ 4.1 (11.2–25.5)
Chlorophyll a ( $\mu$ g L <sup>-1</sup> )	5 $\pm$ 4 (2–17)	25 $\pm$ 26 (3–81)
Fe:Ca molar	0.036 $\pm$ 0.026 (0.007–0.088)	0.002 $\pm$ 0.001 (0.000–0.005)
Fe:P molar	6.0 $\pm$ 2.4 (2.0–13.3)	0.7 $\pm$ 0.6 (0.1–2.3)

### 3.5 Comparison of soil, aquatic sediment, shallow groundwater, and kettle hole water composition

At KR, the PCA, using molar ratio Fe:Ca, Fe:K and Ca:K, revealed that relative Fe, Ca, K compositions of the edge and footslope position resembled that Fe, Ca, K composition of the sediment core (0–2 cm and 5–10 cm) (Fig. S5). Thus, colluvial soils and kettle hole sediments were enriched in Fe relative to Ca and K (Fig. 3). However, the sediment was enriched with Fe by factor 2 ( $EF_{Fe}=2$ ), if compared to the footslope and edge positions, but only by an EF of 1.5 compared to the hilltop and hillslope positions (Fig. 4). Calcium was enriched ( $EF_{Ca}=2$ ), if compared to the footslope position, but was depleted compared to the other slope positions ( $EF_{Ca}=0.2–1$ ). The  $EF_K$  was

**Fig. 3** Radar charts showing the distribution of iron (Fe), calcium (Ca), potassium (K), and total phosphorous (TP) in soils (in  $\text{mg g}^{-1}$ ), kettle hole water (in  $\text{mg L}^{-1}$ ), and sediments (in  $\text{mg g}^{-1}$ ) from Kraatz and Rittgarten. Note that the TP concentration in kettle hole water has been multiplied by the factor of 10 to visualize site-specific differences

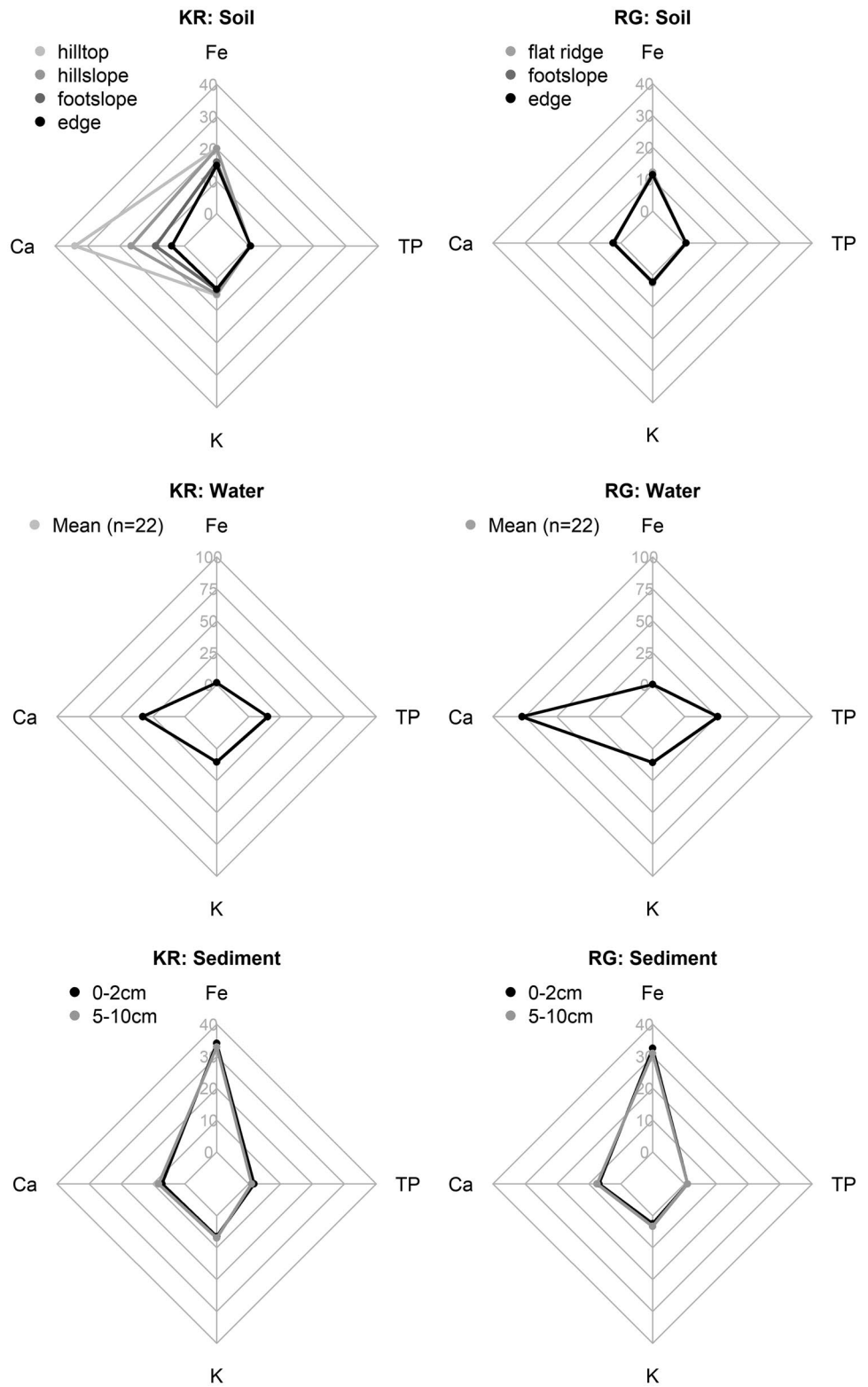
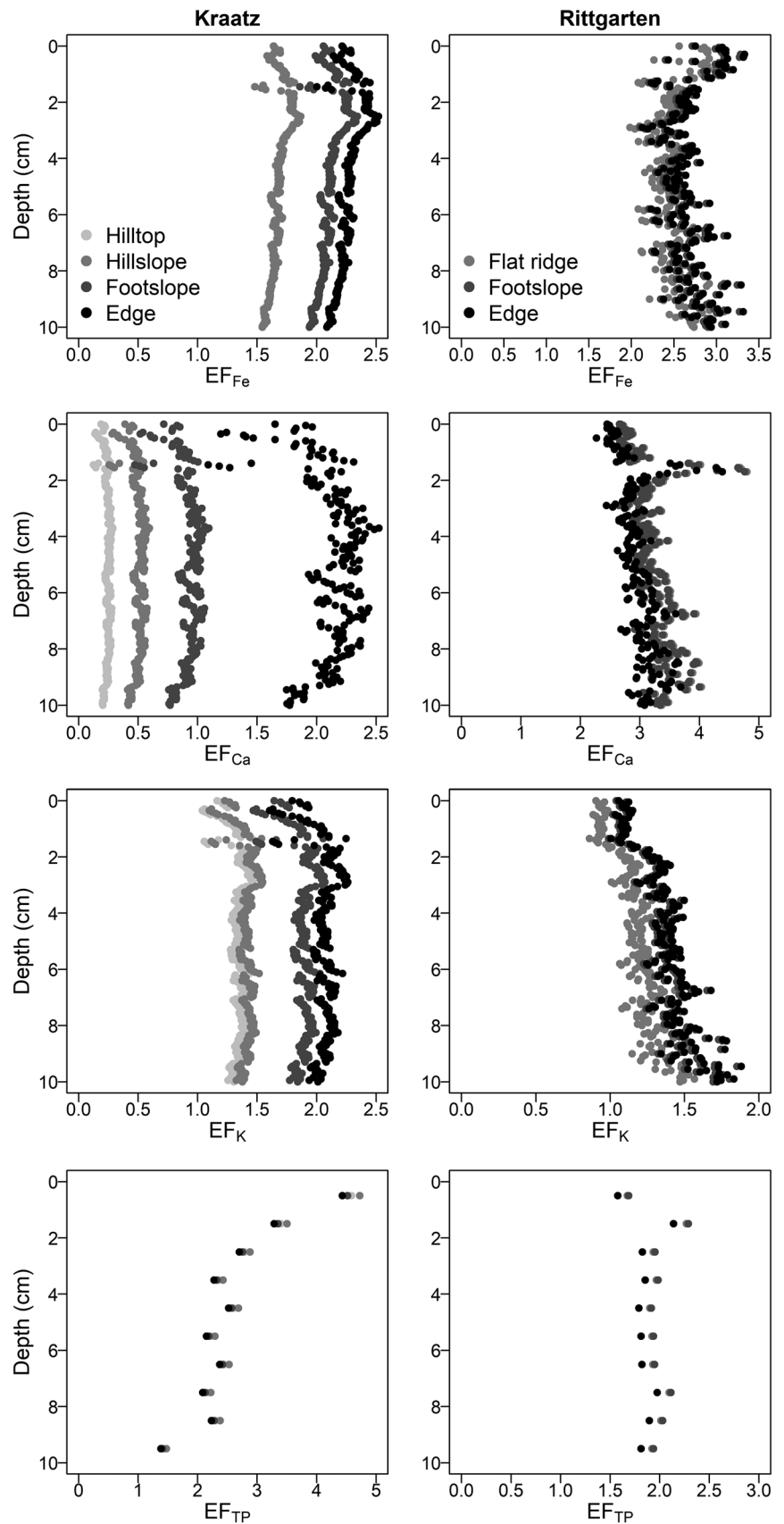




**Fig. 4** Element(X)-specific enrichment factor ( $EF_X$ ) of the sediment core at the Kraatz (left panels) and Rittgarten kettle hole (right panels). TP total P



similar to  $EF_{Fe}$  ( $EF_K = 2$ ) for the footslope and edge positions, but significantly higher for the hilltop and hillslope positions (1–1.5). The  $EF_{TP}$  decreased from 4.7 to 1.4 downward with little variation across all slope positions (hilltop, hillslope, foot slope, edge).

At RG, the relative Fe, Ca, K composition of the soil samples differed from that of the sediment core. Owing to the low variability of the Fe, Ca, and K concentrations of soils (Fig. 2), EF between the different sampling sites were similar. In contrast to KR,  $EF_{Fe}$  was slightly higher (2–3),  $EF_K$  was similar (0.8–2), and  $EF_{Ca}$  was higher (2.8–4.3, except for some higher/lower values) throughout the RG sediment core ( $P < 0.001$ ). In contrast to KR, the  $EF_{TP}$  remained constant around 2.

The relative Fe, Ca, K composition of the kettle hole water and shallow groundwater differed strongly from that of soils and sediments, i.e., the mean annual Fe, Ca, K composition of shallow groundwater (Table 3) and kettle hole water (Table 4) was dominated by Ca followed by K. Due to the dominating geochemical conditions the concentration of  $Fe^{2+}$  is relatively low. Furthermore, the ratio of median kettle hole water Ca concentration over median groundwater concentration was 0.5 and the ratio of median  $HCO_3$  concentration was 0.6 for both KR and RG. The ratio of median kettle hole water K concentration over median groundwater concentration was 0.8 for KR and 1.3 for RG, and the ratio of median Mg concentration was 1.0 for KR and 0.8 for RG.

A Piper diagram was used to reveal certain properties of the total ion relationships between shallow groundwater wells and kettle hole water (Fig. 5). All four KR-GW wells differ due to their ionic composition. Regarding the cations, two groups can be distinguished by higher  $meq\ L^{-1}\%$  of Ca (KR-GW-1 and KR-GW-4). On the other side, groundwater observation wells KR-GW-2 and KR-GW-3 are characterized by clear difference of  $\% meq\ L^{-1}\ HCO_3$  relative to the  $SO_4$ . The kettle hole water lies between the end members of the groundwater clusters, only with slightly shift to higher  $\% meq\ L^{-1}$  of Cl compared to groundwater.

At RG, the main differences occur between the equivalent percentages of the shallow groundwater wells. Two clusters can be distinguished. Observation wells RG-GW-2 and RG-GW-3 are characterized by lower  $HCO_3\% meq\ L^{-1}$  relative to the  $SO_4$ . Wells RG-GW 1 and RG-GW-4, on the other hand, are characterized by higher  $\% meq\ L^{-1}$  of  $HCO_3^-$ . Differentiation of cations only play a minor role. Basically, the kettle hole water lies exactly between the end members of the two shallow groundwater clusters with slightly shift to higher  $\% meq\ L^{-1}$  of K and Cl compared to shallow groundwater. Regarding the cations there is a decrease of  $\% meq\ L^{-1}$  Ca relative to K from shallow groundwater to kettle hole water.

### 3.6 Distribution of erosional and depositional areas and estimation of the eroded material at the Kraatz kettle hole

The trained CUBIST model provided the formula C-horizon depths =  $13 + 15.3 \times TWI - 86 \times TPI - 25$ . The bi-plot of the CUBIST simulated vs. measured/calculated C-horizon depths resulted in an  $R^2$  of 0.88 (Fig. S6) including an estimated error of 40 cm. The spatial distribution of erosion (negative values) and deposition sites (positive amounts) are shown in Fig. 6. Summing all cells, a total volume of  $10,484\ m^3$  was eroded upslopes and  $8428\ m^3$  was deposited downslopes, respectively. This yields a total “missing” volume of  $2,056\ m^3$  of material, which is likely transported from the terrestrial sites into the kettle hole. This accounts for on average 104 cm of kettle hole sediment over the last 100 years (Kleeberg et al. 2016b). This corresponds to the results of a regionally neighboring study (Wilken et al. 2020) in which was calculated that only a small part of the eroded material is deposited in the kettle hole by very few rainfall events and a significantly larger part remains downslopes, in the kettle hole surrounding flat.

## 4 Discussion

### 4.1 Processes in the catchment

Intensive agricultural practices in undulating areas of young moraine landscapes cause erosion by water and tillage and resulting in the redistribution of large amounts of soil material (Sommer et al. 2008; Deumlich et al. 2010; Calitri et al. 2019). After some decades, this process increases the local soil heterogeneity and leads to the development of new soil types that differ in elemental composition (Ellerbrock et al. 2016). In the two shown experimental sites, erosion and deposition processes were ubiquitous, especially at the KR catchment (Fig. 6).

The decrease in Ca, Fe, and K concentrations of soils across the topographic positions at KR (Fig. 2) is in agreement with previously determined elemental concentrations at KR (Leue et al. 2019). Frequent and strong erosion at hilltops and partly at hillslopes has initially exposed the carbon rich A-horizon material, followed by the clay-rich Bt-horizon and, recently, the carbonate-rich glacial till. Today hilltops are characterized by A-C profiles and Calcaric Regosols (caRG) with high  $CaCO_3$  contents throughout the profile (Leue et al. 2019). Erosion of  $CaCO_3$ -Ca rich material at Calcaric Regosols (caRG) and its downslope transport and deposition at lower topographic positions are mirrored in Ca enrichment of surface soil material at foot slopes and edge positions. This is supported by

**Fig. 5** Piper diagrams of anions and cations in individual shallow groundwater (GW) wells at Kraatz (top) between February and June 2014 ( $n=14$  occasions) and at Rittgarten (bottom) between February and May 2014 ( $n=12$  occasions), and in kettle hole water at Rittgarten and Kraatz between July 2013 and July 2014 ( $n=22$  occasions). At both kettle holes, groundwater wells 1 and 4 are located in the inflow and wells 2 and 3 are located in the outflow area

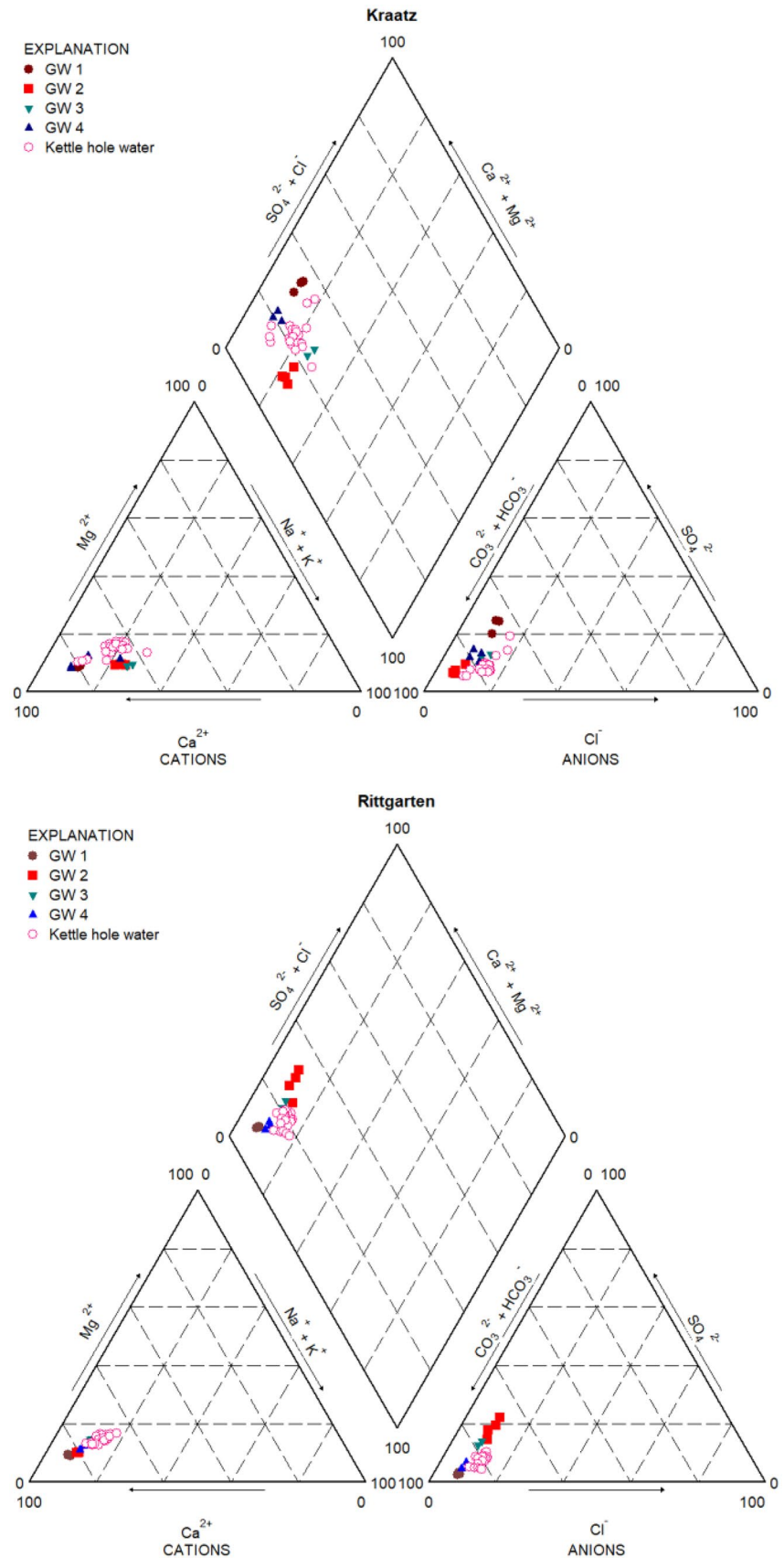
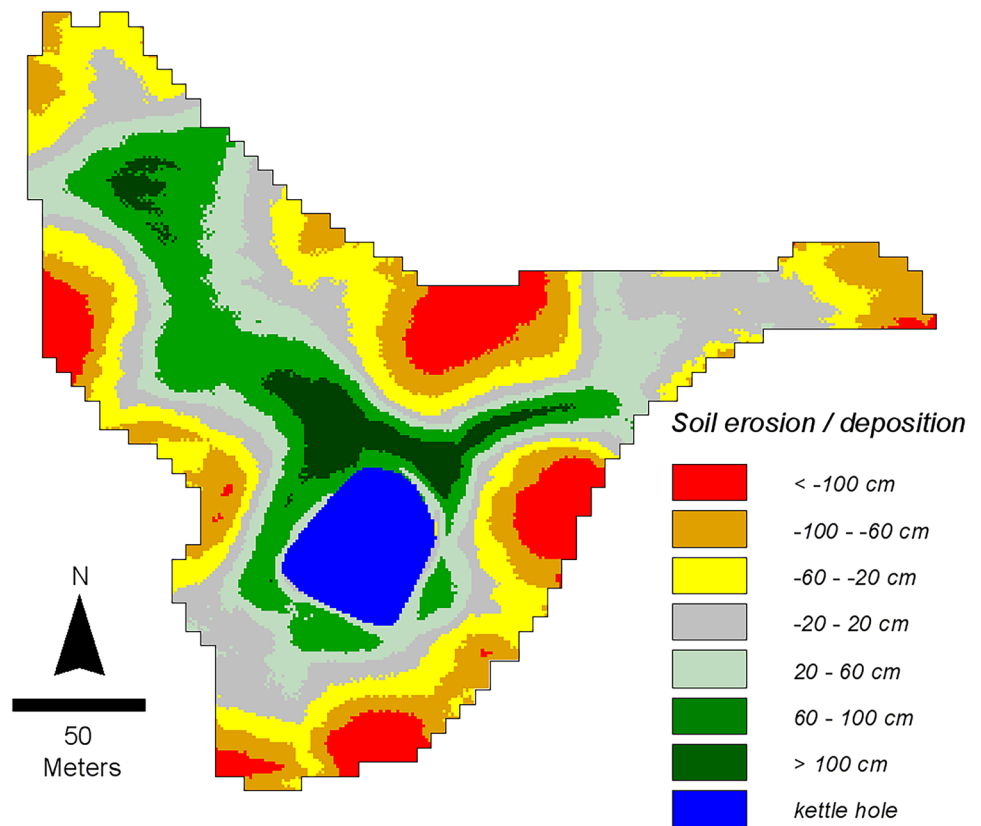


**Fig. 6** Distributions of erosional and depositional areas and estimated eroded or deposited material (in cm) at the Kraatz kettle hole



the significant correlation between Ca and TIC content ( $r=0.99$ ,  $P<0.01$ ). Furthermore, erosion on hillslopes has exposed Bt-horizons, which are rich in clay and therefore also in Fe and K. This profile shortening caused the formation of Calcic Luvisols (eLV) at hillslopes.

At RG, the similar Ca, Fe, and K concentrations across the soil transects (Fig. 2) agree well with the rather uniform soil types mostly comprising of Haplic Luvisol and Colluvic Gleysol (coGG) (Table S1). Thus, it is reasonable to assume that the development of the glacial soil continuum takes more time at RG owing to the relatively flat topography.

Furthermore, two main reasons exist for the rather constant TP content across the soil transects at both sites (Fig. 2). The annual P input by pig slurry exceeded by approximately 50% the balance of P fertilization and crop uptake. Moreover, the P-binding capacity of the soil (OM, Fe, Al, Ca) was insufficient to capture mobile P not taken up by plants. Thus, excess P is being directly and frequently discharged into the kettle holes.

The chemical weathering of the  $\text{CaCO}_3$ -rich glacial till likely caused the high Ca concentrations in shallow groundwater at both sites (Table 3). While glacial till was present at hilltops at KR, no glacial till was found by soil augering up to 1 m depth at RG. Owing to the uniformity of the basic geochemistry of both catchments in the overall glacial Quilow catchments, the occurrence of the glacial till in deeper

soil layers could be suspected. Furthermore, liming and fertilization likely contributed to the Ca, K, and phosphate concentration in shallow groundwater to some extent; however, their contributions to the shallow groundwater are difficult to quantify. The higher concentrations of K and Mg at groundwater measuring points KR-GW-1 and KR-GW-2 could be an indication of the influence of liming in the catchment. These monitoring wells are located in the slope foot zone, where accumulation in the shallow groundwater is likely as a result of K and Mg losses from the soil due to liming (Jaskulska et al. 2014).

#### 4.2 External and internal filter that affect the kettle hole water and sediment biogeochemistry

The elemental composition of the kettle hole water is determined by the elemental composition and amount of inflow, uptake via vegetation (macrophytes) and primary producers, as well as by biogeochemical processes in the water column and in the sediment. Recent studies found strong evidence for at least temporal connection of the kettle holes in the Quilow catchment to a shallow groundwater system (Lischeid et al. 2017; Kayler et al. 2018) including the two kettle holes in this study (Nitzsche et al. 2017a; Vyse et al. 2020).

The high Ca, Mg, and  $\text{HCO}_3$  concentrations in the kettle hole water is due to shallow groundwater input. Comparing

the ionic composition of the two shallow groundwater clusters and the kettle hole water (Fig. 5), the flow direction of groundwater was assessed. At RG, a flow through from SE (observation wells RG-GW-1 and RG-GW-4) to NW (observation wells RG-GW-2 and RG-GW-3) direction is expected. Inorganic or biogenic calcite precipitation is a common process in Ca-rich lake ecosystems especially following phytoplankton blooms (Heine et al. 2017) and was previously suggested for the KR and RG kettle holes (Kleeberg et al. 2016a). Thus, the lower Ca and  $\text{HCO}_3^-$  concentrations at wells RG-GW-2 and RG-GW-3 can be interpreted as a direct influence of the kettle hole water. Furthermore, the relative shift from Ca to K from shallow groundwater to kettle hole water could be due to the microbial decomposition of OM in surface waters (Klink 2005). Oxic kettle hole water lowers the potential of  $\text{SO}_4$  reduction in the groundwater wells RG-GW-2 and RG-GW-3 located in the expected groundwater downstream area. At KR and although the Ca and  $\text{HCO}_3^-$  concentrations of KR-GW-1 and KR-GW-2 are higher compared to KR-GW-3 and KR-GW-4, the ionic composition of KR-GW-1 and KR-GW-4 shows higher comparability (Fig. 5). Therefore, a flow direction of groundwater from NE (observation wells 1 and 4) in direction SW (KR-GW 2 and 3) is plausible. These observations coincide with measurements of the hydraulic gradients at the shallow groundwater monitoring sites during 2014 and measurement of stable isotopes of oxygen ( $\delta^{18}\text{O}$ ) and hydrogen ( $\delta\text{D}$ ) in 2015 and 2016 (Vyse et al. 2020). Thus, the kettle hole water quality is closely related to that of the shallow groundwater body, while the groundwater quality of the groundwater outflow is directly impacted by kettle hole internal processes.

Furthermore, Fe, Ca, K and P are key nutrients for macrophytes, and biological uptake could lead to lower elemental concentrations in the kettle hole water compared to the shallow groundwater. Some *Lemna* spp. were found to remove N, P, K, Mg, and Ca from wastewater (Patel and Kanungo 2010; Showqi et al. 2017). If we apply elemental concentrations previously determined in *Lemna* dry weight (Balasubramanian and Kasturi Bai 1992), the area of floating duckweed (*Lemna minor*, *Spirodela polyrhiza*) of the water surface in June, and the biomass of duckweed (Kazanjian et al. 2018), then the amount of Ca, K, and P present in duckweed was about 40 times higher in RG than in KR (Table S2). While these are only rough estimates that could change based on the elemental concentrations of the duckweed, these numbers can help to understand differences in the elemental enrichment across different sites. Thus, *Lemna* (and other macrophytes) likely accumulated Ca, K, and P (and Fe) from the kettle hole water, functioning as an intermediate storage phase.

Furthermore, anoxic conditions usually prevail from May to August (Kazanjian et al. 2018), which might lead in RG to the formation of insoluble  $\text{FeS}_x$ . Consequently,  $\text{Fe}^{2+}$  could become depleted in the water column, which is well in

agreement with the lower Fe concentration in RG compared to KR. During oxic conditions, ferrous iron ( $\text{Fe}^{2+}$ ) is oxidized to ferric iron ( $\text{Fe}^{3+}$ ) and immediately precipitate as Fe hydroxide. These Fe-bearing minerals such as  $\text{FeOOH}/\text{Fe}(\text{OH})_3$  can bind P and therefore control the TP concentration in the water column (Kleeberg et al. 2016a). The higher molar Fe:P ratio in the water of KR (6.0, span: 2.0–13.3) than that of RG (0.7, span: 0.1–2.3) agrees well with the molar Fe:P ratio in the entrapped sediment material (Kleeberg et al. 2016a). Thus, the Fe:P ratio in kettle hole water supports the general conclusion made by Kleeberg et al. (2016a) that a higher Fe:P ratio indicates redox-dependent Fe–P binding at KR, while low  $\text{Fe}^{2+}$  concentration due to  $\text{FeS}_x$  precipitation at RG hamper the Fe–P binding. As the water column and sediment are in close contact, these internal processes in the water column are prone to directly affect the element composition of the sediment.

The present study only focused on the top 10 cm of a  $\text{Cs}^{137}/\text{Pb}^{210}$  dated sediment (Kleeberg et al. 2016b) that represents material recently deposited, i.e. at KR between 1993 to 2013, and at RG between 1965 to 2013. The PCA revealed that the top 10 cm sediment of the KR kettle hole tended to reflect the Fe, Ca, K composition of the soil from the foot-slope and edge positions (Fig. S5), and thus element-specific input via erosion (see below). As the top 10 cm sediment of the RG kettle hole was not in good agreement with the surrounding soils, external filters in the catchment or internal filters in the kettle hole water must exist which explain this imbalance. These filters could also explain the elemental enrichment compared to the near kettle hole agricultural soils (Fig. 4).

Firstly, macrophytes could contribute to the elemental enrichment. Following die off, macrophytes are prone to sedimentation. Owing to the high abundance at RG, sedimentation of duckweed may partly explain the higher elemental EF at RG compared to KR. Secondly, Ca could become enriched via calcite formation. Furthermore, co-precipitation of biogenic hydroxyapatite ( $\text{Ca}_5(\text{PO}_4)_3\text{OH}$ ) (Boyd 2015) could lead to the enrichment of P in the sediment as previously suggested (Kleeberg et al. 2016b). Thirdly, the formation of insoluble  $\text{FeS}_x$  could contribute to the Fe enrichment in the sediment as previously suspected for RG (Kleeberg et al. 2016a, b). On the other hand, Fe-bearing minerals such as  $\text{FeOOH}$  formed during oxic phases at KR could bind with P and lead to the enrichment of Fe and TP at KR (Kleeberg et al. 2016b).

Furthermore, the deposition of soil particles and application of fertilizers could lead to the enrichment in sediments. Previous studies found the enrichment of elements with decreasing particle size. For example, iron was enriched in clay-sized particles ( $< 2 \mu\text{m}$ ) that contain as Fe (hydr)oxides (Asano and Wagai 2014) and P was enriched in clay-sized particles of subtropical red soils (Li et al. 2016). Nutrients (Mg, Ca, TP, K) were also associated with the very fine sediment fraction



(< 16  $\mu\text{m}$ ) in sediments from retention ponds (Verstraeten and Poesen 2002). Nitzsche et al. (2017b) found the sediment horizon from 2 to 7 cm at KR was dominated by clay and silt sized particles. Thus, it is reasonable to assume the deposition of these fine particles contributed to the enrichment of Fe, Ca, K, and TP in the kettle hole sediment. Furthermore, K and TP could have originated from the pig slurry that was applied since approximately 1990, and Ca from liming until 2010. When subtracting the annual mass of elements removed by crops per hectare (in  $\text{ha}^{-1} \text{year}^{-1}$ ) from the slurry mass applied and scaling to the catchment area, then an excess of approximately 50 kg TP, 160 kg K, and 1300 kg Ca per year is potentially transported into both kettle holes via surface runoff and subsurface flow. Thus, the application of these fertilizers could have contributed to the enrichment of Ca, K, and TP in the surface sediment.

### 4.3 Long-term consequences for kettle holes

Loss of elements from soils to kettle holes has negative consequences for both farming (high heterogeneity of soil nutrient conditions at arable fields) and the trophic state of kettle holes. Water and tillage erosion increase the spatial soil heterogeneity including elemental composition and soil texture with strong local effects on soil productivity (Figs. 2 and 6). As a consequence, farmers have increasing difficulties to adjust the crop-specific nutrient demand via fertilization that may lead to over-fertilization for the whole field. The annual P input exceeded P removal leading to excess P that is discharged into the kettle hole and may lead to their eutrophication (Kleeberg et al. 2016b; Kazanjian et al. 2018). Studies of P erosion have suggested reducing P inputs to maintain a clean water status (Schippers et al. 2006; Alewell et al. 2020). Schippers et al. (2006) found exactly the same P surplus as we did (Table 2) and consider a reduction from 15 to 0.7  $\text{kg ha}^{-1} \text{year}^{-1}$  as a prerequisite for a permanent clean water status. Overall, the kettle hole in the Quillow region belong to aquatic systems which are enriched in P (eutrophication) mostly due to intensive agricultural production in their catchment area (Lischeid and Kalettka 2012). The concentration of TP (KR: 0.041–0.373  $\text{mg L}^{-1}$ ; RG: 0.033–1.095  $\text{mg L}^{-1}$ , Table 4) is within the range of TP for kettle holes in Brandenburg, Germany (0.01–3  $\text{mg L}^{-1}$ , Fig. S7). These concentrations also fall within the range of eutrophic (0.016–0.386  $\text{mg L}^{-1}$ ) and hypereutrophic lakes (0.75–1.2  $\text{mg L}^{-1}$ ) (Wetzel 2001).

We expect that other kettle holes in intensively managed agricultural landscapes of NE Germany and globally are similarly negatively impacted by soil elemental inputs from the surrounding catchment. Thus, we strongly advise land management practices (tillage and fertilization) to be carefully adjusted to the crop-specific demand in order to reduce soil and nutrient input into kettle holes.

## 5 Conclusions

The biogeochemistry of small-volume aquatic systems is strongly, i.e., directly and indirectly, influenced by their terrestrial catchments. In an area with short and steep slopes (KR) large amounts of soil material can be redistributed from hill-tops to footslopes, kettle hole edges, and especially into the water body. The dominance of material input through erosion is a combination of geomorphological conditions, water erosion, and agricultural cultivation. Soil erosion and deposition processes lead to a selective or element-specific mobilization, transport, and long-term burial in aquatic sediments. Shallow groundwater input is an important elemental transportation and entry path but can also lead to a dilution of nutrients and pollutants under the given flow conditions.

The dominant plant community, adapted to the elemental input, can selectively delay element (e.g., Ca) burial in the kettle hole sediment. The considerable element losses from the surrounding soils and subsequent inputs into the kettle hole represents a large unidirectional flux of nutrients and reactive material that should be countered with comprehensive soil protection measures in the interest of soil and water protection.

**Supplementary information** The online version contains supplementary material available at <https://doi.org/10.1007/s11368-022-03145-8>.

**Acknowledgements** We are grateful to all persons who have contributed to this study. Dorith Henning, Roswitha Schulz and Joachim Bartelt (†) (all Leibniz-Centre for Agricultural Landscape Research ZALF, Institute of Landscape Hydrology, LWH) regularly sampled the kettle holes. Rita Schwarz (†), Melitta Engel (both ZALF, LWH) and Kristina Holz (ZALF, Central Laboratory) conducted most of the laboratory analysis. Gernot Verch (ZALF) provided information on the land management. We kindly thank the LandScales team for their support and discussions.

**Funding** This research was funded through the Pact for Innovation and Research of the Gottfried Wilhelm Leibniz association (project LandScales—‘Connecting processes and structures driving landscape carbon dynamics over scales’) (SAW-2012-ZALF-3).

**Data Availability** The research data are available from the BonaRes Repository : <https://doi.org/10.20387/bonares-9bbk-z07e>.

**Code Availability** Not applicable.

## Declarations

**Conflict of interest** The authors declare no competing interests.

## References

- Alewell C, Ringeval B, Ballabio C et al (2020) Global phosphorus shortage will be aggravated by soil erosion. *Nat Commun* 11:1–12. <https://doi.org/10.1038/s41467-020-18326-7>



- Andersen JM (1976) An ignition method for determination of total phosphorus in lake sediments. *Water Res* 10:329–331. [https://doi.org/10.1016/0043-1354\(76\)90175-5](https://doi.org/10.1016/0043-1354(76)90175-5)
- Asano M, Wagai R (2014) Evidence of aggregate hierarchy at micro- to submicron scales in an allophanic andisol. *Geoderma* 216:62–74. <https://doi.org/10.1016/j.geoderma.2013.10.005>
- Attermeyer K, Grossart HP, Flury S, Premke K (2017) Bacterial processes and biogeochemical changes in the water body of kettle holes - mainly driven by autochthonous organic matter? *Aquat Sci* 79:675–687. <https://doi.org/10.1007/s00027-017-0528-1>
- Balasubramanian PR, Kasturi Bai R (1992) Recycling of biogas-plant effluent through aquatic plant (*Lemna*) culture. *Bioresour Technol* 41:213–216. [https://doi.org/10.1016/0960-8524\(92\)90004-H](https://doi.org/10.1016/0960-8524(92)90004-H)
- Biddanda BA, Cotner JB (2002) Love handles in aquatic ecosystems: The role of dissolved organic carbon drawdown, resuspended sediments, and terrigenous inputs in the carbon balance of Lake Michigan. *Ecosystems* 5:431–445. <https://doi.org/10.1007/s10021-002-0163-z>
- Boyd CE (2015) Phosphorus. *Water Quality*, 2nd edn. Springer, Cham, pp 243–261
- Branco BF, Torgersen T (2009) Diurnal sediment resuspension and settling: Impact on the coupled physical and biogeochemical dynamics of dissolved oxygen and carbon in a shallow water body. *Mar Freshw Res* 60:669–679. <https://doi.org/10.1071/MF08113>
- Brenner M, Binford MW (1988) Relationships between concentrations of sedimentary variables and trophic state in Florida lakes. *Can J Fish Aquat Sci* 45:294–300. <https://doi.org/10.1139/f88-035>
- Calitri F, Sommer M, Norton K et al (2019) Tracing the temporal evolution of soil redistribution rates in an agricultural landscape using  $^{239+240}\text{Pu}$  and  $^{10}\text{Be}$ . *Earth Surf Process Landforms* 44:1783–1798. <https://doi.org/10.1002/esp.4612>
- Deumlich D, Funk R, Frielinghaus M et al (2006) Basics of effective erosion control in German agriculture. *J Plant Nutr Soil Sci* 169:370–381. <https://doi.org/10.1002/jpln.200621983>
- Deumlich D, Schmidt R, Sommer M (2010) A multiscale soil-landform relationship in the glacial-drift area based on digital terrain analysis and soil attributes. *J Plant Nutr Soil Sci* 173:843–851. <https://doi.org/10.1002/jpln.200900094>
- Ellerbrock RH, Gerke HH, Deumlich D (2016) Soil organic matter composition along a slope in an erosion-affected arable landscape in North East Germany. *Soil Tillage Res* 156:209–218. <https://doi.org/10.1016/j.still.2015.08.014>
- Farkas C, Beldring S, Bechmann M, Deelstra J (2013) Soil erosion and phosphorus losses under variable land use as simulated by the INCA-P model. *Soil Use Manag* 29:124–137. <https://doi.org/10.1111/j.1475-2743.2012.00430.x>
- Frielinghaus M, Vahrson W-G (1998) Soil translocation by water erosion from agricultural cropland into wet depressions (morainic kettle holes). *Soil Tillage Res* 46:23–30. [https://doi.org/10.1016/S0167-1987\(98\)80104-9](https://doi.org/10.1016/S0167-1987(98)80104-9)
- Gaspar L, Lizaga I, Navas A (2020) Elemental mobilisation by sheet erosion affected by soil organic carbon and water fluxes along a radiotraced soil catena with two contrasting parent materials. *Geomorphology* 370:107387. <https://doi.org/10.1016/j.geomorph.2020.107387>
- Gericke A, Kiesel J, Deumlich D, Venohr M (2019) Recent and future changes in rainfall erosivity and implications for the soil erosion risk in Brandenburg. NE Germany *Water* 11:904. <https://doi.org/10.3390/w11050904>
- Gołdyn B, Chudzińska M, Barańkiewicz D, Celewicz-Goldyn S (2015) Heavy metal contents in the sediments of astatic ponds: Influence of geomorphology, hydroperiod, water chemistry and vegetation. *Ecotoxicol Environ Saf* 118:103–111. <https://doi.org/10.1016/j.ecoenv.2015.04.016>
- Haygarth PM, Delgado A, Chardon WJ et al (2013) Phosphorus in soils and its transfer to water: from fine-scale soil processes to models and solutions in landscapes and catchments. *Soil Use Manag* 29:1–5. <https://doi.org/10.1111/sum.12036>
- Heine I, Brauer A, Heim B et al (2017) Monitoring of calcite precipitation in hardwater lakes with multi-spectral remote sensing archives. *Water* 9:15. <https://doi.org/10.3390/w9010015>
- IUSS Working Group WRB (2015) World Reference Base for Soil Resources 2014, update 2015. International soil classification system for naming soils and creating legends for soil maps. World Soil Resources Reports No. 106. FAO, Rome
- Jaskulska I, Jaskulski D, Kobierski M (2014) Effect of liming on the change of some agrochemical soil properties in a long-term fertilization experiment. *Plant, Soil Environ* 60:146–150. <https://doi.org/10.17221/850/2013-pse>
- Kaletka T, Rudat C (2006) Hydrogeomorphic types of glacially created kettle holes in North-East Germany. *Limnologica* 36:54–64. <https://doi.org/10.1016/j.limno.2005.11.001>
- Kaletka T, Rudat C, Quast J (2001) “Potholes” in Northeast German agro-landscapes: functions, land use impacts, and protection strategies. In: Tenhunen JD, Lenz R, Hantschel R (eds) *Ecosystem Approaches to Landscape Management in Central Europe*. Springer, Berlin, pp 291–298
- Kayler ZE, Badrian M, Frackowski A et al (2018) Ephemeral kettle hole water and sediment temporal and spatial dynamics within an agricultural catchment. *Ecohydrology* 11:e1929. <https://doi.org/10.1002/eco.1929>
- Kazanjian G, Flury S, Attermeyer K et al (2018) Primary production in nutrient-rich kettle holes with differing plant communities and consequences for nutrient and carbon cycling. *Hydrobiologia* 806:77–93. <https://doi.org/10.1007/s10750-017-3337-6>
- Kleeberg A, Herzog C, Jordan S, Hupfer M (2010) What drives the evolution of the sedimentary phosphorus cycle? *Limnologica* 40:102–113. <https://doi.org/10.1016/j.limno.2009.11.001>
- Kleeberg A, Neyen M, Kaletka T (2016a) Element-specific downward fluxes impact the metabolism and vegetation of kettle holes. *Hydrobiologia* 766:261–274. <https://doi.org/10.1007/s10750-015-2460-5>
- Kleeberg A, Neyen M, Schkade U-K et al (2016b) Sediment cores from kettle holes in NE Germany reveal recent impacts of agriculture. *Environ Sci Pollut Res* 23:7409–7424. <https://doi.org/10.1007/s11356-015-5989-y>
- Klink A (2005) Chemical changes and nutrient release during decomposition processes of mature leaves of *Nuphar lutea* (L.) Sibth. & Sm under laboratory conditions. *Ecohydrology* 5:215–222
- Leue M, Hoffmann C, Hierold W, Sommer M (2019) In-situ multi-sensor characterization of soil cores along an erosion-deposition gradient. *CATENA* 182:104140. <https://doi.org/10.1016/j.catena.2019.104140>
- Li B, Ge T, Xiao H et al (2016) Phosphorus content as a function of soil aggregate size and paddy cultivation in highly weathered soils. *Environ Sci Pollut Res* 23:7494–7503. <https://doi.org/10.1007/s11356-015-5977-2>
- Li Y, Yu S, Strong J, Wang H (2012) Are the biogeochemical cycles of carbon, nitrogen, sulfur, and phosphorus driven by the “Fe<sup>III</sup>-Fe<sup>II</sup> redox wheel” in dynamic redox environments? *J Soils Sediments* 12:683–693. <https://doi.org/10.1007/s11368-012-0507-z>
- Lischeid G, Balla D, Dannowski R et al (2017) Forensic hydrology: what function tells about structure in complex settings. *Environ Earth Sci* 76:40. <https://doi.org/10.1007/s12665-016-6351-5>
- Lischeid G, Kaletka T (2012) Grasping the heterogeneity of kettle hole water quality in Northeast Germany. *Hydrobiologia* 689:63–77. <https://doi.org/10.1007/s10750-011-0764-7>
- Lischeid G, Kaletka T, Holländer M et al (2018) Natural ponds in an agricultural landscape: External drivers, internal processes, and the role of the terrestrial-aquatic interface. *Limnologica* 68:5–16. <https://doi.org/10.1016/j.limno.2017.01.003>

- Menzel RG (1980) Enrichment ratios of water quality modelling. In: Knisel WG (ed) CREAMS - a field scale model for chemicals, runoff and erosion from agricultural management systems. US Department of Agriculture, Conservation Research Report No. 26, pp 486–492
- Neyen M (2014) Depositional characteristics of glacial kettle holes at Kraatz and Rittgarten, NE Brandenburg, Germany. Bachelor Thesis, University of Potsdam
- Nitzsche KN, Kaiser M, Premke K et al (2017b) Organic matter distribution and retention along transects from hilltop to kettle hole within an agricultural landscape. *Biogeochemistry* 136:47–70. <https://doi.org/10.1007/s10533-017-0380-3>
- Nitzsche KN, Kalettka T, Premke K et al (2017a) Land-use and hydroperiod affect kettle hole sediment carbon and nitrogen biogeochemistry. *Sci Total Environ* 574:46–56. <https://doi.org/10.1016/j.scitotenv.2016.09.003>
- Nitzsche KN, Verch G, Premke K et al (2016) Visualizing land-use and management complexity within biogeochemical cycles of an agricultural landscape. *Ecosphere* 7:e01282. <https://doi.org/10.1002/ecs2.1282>
- Onandia G, Lischeid G, Kalettka T et al (2018) Biogeochemistry of natural ponds in agricultural landscape: lessons learned from modeling a kettle hole in Northeast Germany. *Sci Total Environ* 634:1615–1630. <https://doi.org/10.1016/j.scitotenv.2018.04.014>
- Patel D, Kanungo V (2010) Phytoremediation potential of duckweed (*Lemna minor* L: a tiny aquatic plant) in the removal of pollutants from domestic wastewater with special reference to nutrients. *The Bioscan* 5:355–358
- Prasad M, Greger M, Aravind P (2005) Biogeochemical Cycling of Trace Elements by Aquatic and Wetland Plants. In: Prasad MNV, Sajwan KS, Naidu R (eds) Trace Elements in the Environment - Biogeochemistry, Biotechnology, and Bioremediation. Taylor & Francis, Boca Raton, pp 443–474
- Premke K, Attermeyer K, Augustin J et al (2016) The importance of landscape complexity for carbon fluxes on the landscape level: Small-scale heterogeneity matters. *Wires Water* 3:601–617. <https://doi.org/10.1002/wat2.1147>
- Reverey F, Ganzert L, Lischeid G et al (2018) Dry-wet cycles of kettle hole sediments leave a microbial and biogeochemical legacy. *Sci Total Environ* 627:985–996. <https://doi.org/10.1016/j.scitotenv.2018.01.220>
- Schippers P, van de Weerd H, de Klein J et al (2006) Impacts of agricultural phosphorus use in catchments on shallow lake water quality: About buffers, time delays and equilibria. *Sci Total Environ* 369:280–294. <https://doi.org/10.1016/j.scitotenv.2006.04.028>
- Showqi I, Ahmad Lone F, Ahmad Bhat JI (2017) Evaluation of the efficiency of duckweed (*Lemna minor* L.) as a phytoremediation agent in wastewater treatment in Kashmir Himalayas. *J Bioremediation Biodegrad* 8:405. <https://doi.org/10.4172/2155-6199.1000405>
- Sommer M, Gerke HH, Deumlich D (2008) Modelling soil landscape genesis — A “time split” approach for hummocky agricultural landscapes. *Geoderma* 145:480–493. <https://doi.org/10.1016/j.geoderma.2008.01.012>
- Tiner RW (2003) Geographically isolated wetlands of the United States. *Wetlands* 23:494–516. [https://doi.org/10.1672/0277-5212\(2003\)023\[0494:GIWOTU\]2.0.CO;2](https://doi.org/10.1672/0277-5212(2003)023[0494:GIWOTU]2.0.CO;2)
- van der Kamp G, Hayashi M (2009) Groundwater-wetland ecosystem interaction in the semiarid glaciated plains of North America. *Hydrogeol J* 17:203–214. <https://doi.org/10.1007/s10040-008-0367-1>
- Verstraeten G, Poesen J (2002) Regional scale variability in sediment and nutrient delivery from small agricultural watersheds. *J Environ Qual* 31:870–879. <https://doi.org/10.2134/jeq2002.0870>
- Vyse SA, Semiromi MT, Lischeid G, Merz C (2020) Characterizing hydrological processes within kettle holes using stable water isotopes in the Uckermark of Northern Brandenburg, Germany. *Hydrol Process* 34:1868–1887. <https://doi.org/10.1002/hyp.13699>
- Wetzel R (2001) *Limnology*. Academic Press, San Diego, CA
- Wilken F, Ketterer M, Koszinski S et al (2020) Understanding the role of water and tillage erosion from 239+240Pu tracer measurements using inverse modelling. *SOIL* 6:549–564. <https://doi.org/10.5194/soil-6-549-2020>

**Publisher's Note** Springer Nature remains neutral with regard to jurisdictional claims in published maps and institutional affiliations.

## Authors and Affiliations

Kai Nils Nitzsche<sup>1,9</sup>  · Andreas Kleeberg<sup>2</sup> · Carsten Hoffmann<sup>1</sup> · Christoph Merz<sup>1,3</sup> · Katrin Premke<sup>4,10</sup> · Arthur Gessler<sup>5,6</sup> · Michael Sommer<sup>1,7</sup> · Zachary E. Kayler<sup>8</sup>

<sup>1</sup> Leibniz Centre for Agricultural Landscape Research (ZALF), Eberswalder Str. 84, 15374 Muencheberg, Germany

<sup>2</sup> State Laboratory Berlin-Brandenburg, Rudower Chaussee 39, 12489 Berlin, Germany

<sup>3</sup> Hydrogeology Group, Institute of Geological Sciences, Freie Universität Berlin, Malteserstr. 74-100, 12249 Berlin, Germany

<sup>4</sup> Chemical Analytics and Biogeochemistry, Leibniz-Institute of Freshwater Ecology and Inland Fisheries (IGB), Mueggelseedamm 310, 12587 Berlin, Germany

<sup>5</sup> Swiss Federal Institute for Forest, Snow and Landscape Research (WSL), Zuercherstrasse 111, 8903 Birmensdorf, Switzerland

<sup>6</sup> Institute of Terrestrial Ecosystems, ETH Zurich, 8092 Zuerich, Switzerland

<sup>7</sup> Institute of Environmental Science & Geography, University of Potsdam, Karl-Liebknecht-Straße 24-25, 14476 Potsdam, Germany

<sup>8</sup> Department of Soil and Water Systems, University of Idaho, Moscow, ID 83844, USA

<sup>9</sup> Present Address: Biogeochemistry Research Center, Japan Agency for Marine-Earth Science and Technology (JAMSTEC), 2-15 Natsushima-cho, Yokosuka, Kanagawa 237-0061, Japan

<sup>10</sup> Present Address: Charité – Universitätsmedizin Berlin, Charitéplatz 1, 10117 Berlin, Germany